Thermal Concentration Fluctuations of Block Polymer/Homopolymer Mixtures in the Disordered State. 1. Binary Mixtures of SI/HS

Hideaki Tanaka† and Takeji Hashimoto*

Department of Polymer Chemistry, Kyoto University, Kyoto 606, Japan

Received November 6, 1990; Revised Manuscript Received May 6, 1991

ABSTRACT: Small-angle X-ray scattering from binary mixtures of poly(styrene-*block*-isoprene) block copolymer (SI) and homopolystyrene (HS) in the disordered state was studied as a function of degree of polymerization (N_{HS}) and the volume fraction of HS (ϕ_{HS}). The SAXS profiles were compared with the theoretical scattering profiles based on the mean-field random-phase approximation, which incorporates the effects of the asymmetry of monomer volumes and the polydispersity in molecular weights. The theoretical profiles were found to fit the experimental profiles. The best fits of the profiles gave the Flory interaction parameter χ as a function of temperature T, N_{HS}, and ϕ_{HS}. The value χ was found to increase systematically with increasing $1/T$ and ϕ_{HS} and decreasing N_{HS}.

I. Introduction

Small-angle X-ray scattering (SAXS) and small-angle neutron scattering (SANS) from block copolymers have been studied to investigate nature of thermal composition fluctuations occurring in the single-phase state.[1-11] Experimentally obtained SAXS and SANS profiles were compared with the theoretical scattering profiles derived on the basis of the random-phase approximation (RPA),[12,13] which served as a critical test of RPA and provided a method for precise determinations of the Flory interaction parameter χ as a function of the temperature[2,3] T, the degree of polymerization[14] (DP) N, the composition of one block in the copolymer[5,14] f, and the molecular architecture such as the number of arms n in the star-shaped block copolymers.[6,8] The comparison also yielded a method to determine the order–disorder transition (or microphase transition) temperature and the mean-field spinodal temperature for poly(styrene-*block*-isoprene) (SI) or poly(styrene-*block*-butadiene) (SB) type block copolymers.[6,8,14,15]

In this work we extended the studies as described above to binary mixtures of an SI polymer having a given N and f with homopolystyrenes (HS) having various DP (N_{HS}). We pursued a critical test of the scattering theory based upon the RPA, and determined χ as a function of T, N_{HS}, and $\phi_{HS} = 1 - \phi_{SI}$, where ϕ_{SI} and ϕ_{HS} are the volume fractions of SI and HS in the mixtures. A series of work on ordered microdomain structure for the binary mixtures was reported in companion papers.[16,17]

II. Experimental Methods

Table I summarizes the polymers used in this study, where SI and a series of HS (S17, S10, S04, S02, and S01) were prepared by living anionic polymerization as described in detail elsewhere.[17] The SI used here is identical with the copolymer denoted previously[17] by the symbol HY-8, and S stands for HS and the two digits after S denote their M_n (the number-average molecular weight) in unit of thousands.

SI and the binary mixtures SI/HS have rather high order–disorder transition temperatures T_{ODT}. In order to lower T_{ODT} and to enlarge the temperature range where SI and SI/HS are in the disordered state, we added to the systems a relatively small amount of dioctyl phthalate (DOP) as a neutral solvent. We designate the system SI/HS/DOP as SI/HS $(1 - W_{HS})$/$W_{HS}(\phi_P)$ where $1 - W_{HS}$ and W_{HS} denote respectively the weight fractions of SI and HS in the polymer mixture and ϕ_P is the volume of SI plus HS relative to the volume of the system SI/HS/DOP.

The total polymer volume fractions ϕ_P used are 0.66, 0.74, and 0.85, depending on the composition of SI $(1 - W_{HS})$ and HS (W_{HS}) in the polymer mixture SI/HS and molecular weight of HS (M_{HS}) (see Table II). The DOP concentration $(1 - \phi_P)$ was limited to such a small level that the volume fraction of SI, $\phi_P(1 - \phi_{HS})$, in the system SI/HS/DOP is much greater than the corresponding overlap volume concentration $\phi_{C,SI}$ estimated by $\phi_{C,SI} = N_{SI}^{-(3\nu-1)}$ where ϕ_{HS} is the volume fraction of HS ($\phi_{HS} \simeq W_{HS}$), N_{SI} is the

Table I
Characteristics of Polymers Used in This Study

specimen	$10^{-3}M_n$[a]	S/I, w/w %[b]	M_w/M_n[c]
SI	31.6	48/52	1.07
S17	16.7	100/0	1.02
S10	10.2	100/0	1.02
S04	4.4	100/0	1.06
S02	2.3	100/0	1.10
S01	0.9	100/0	1.10

[a] Determined by membrane osmometry or vapor pressure osmometry. [b] Determined by elemental analysis. [c] Determined by size-exclusion chromatography.

Table II
Characteristic Parameters Extracted from SAXS of the Disordered State

sample	comp, w/w %	total polymer conc, vol %	temp range measd, °C	spacing D_S, nm[a]	spacing D_{ST}, nm[b]	spacing D_S/D_{ST}
SI	100/0	66	160–190	23.3 ± 0.4	19.3	1.20
SI/S01	80/20	74	140–170	23.1 ± 0.3	19.3	1.19
	50/50	74	80–110	23.0 ± 0.3	19.4	1.19
	20/80	85	30–60	24.3 ± 0.4	20.4	1.19
SI/S02	80/20	74	140–200	24.1 ± 0.3	19.4	1.24
	65/35	75	110–160	23.8 ± 0.3	19.6	1.21
	50/50	85	160–190	25.0 ± 0.4	20.0	1.25
	35/65	85	160–180	25.4 ● 0.5	20.9	1.21
	20/80	85	130–150	28.3 ± 0.4	23.6	1.20
SI/S04	80/20	66	130–170	23.7 ± 0.3	19.7	1.20
	50/50	66	120–150	26.1 ± 0.5	21.3	1.22
SI/S10	80/20	66	140–170	24.7 ± 0.4	20.7	1.19
	50/50	66	140–180	29.4 ± 0.5	25.4	1.16
SI/S17	80/20	66	140–170	26.9 ± 0.5	22.2	1.21
	50/50	66	140–170	36.7 ± 1.0	32.3	1.14

[a] The value D_s for a given system was independent of temperature and only an averaged value for those estimated at various temperatures is shown (eq 2). [b] Theoretically predicted spacing (eq 7).

† Present address: Mitsubishi Kasei Corp., Research Center, 1000 Kamoshida-cho, Midori-ku, Yokohama 227, Japan.

0024-9297/91/2224-5398$02.50/0

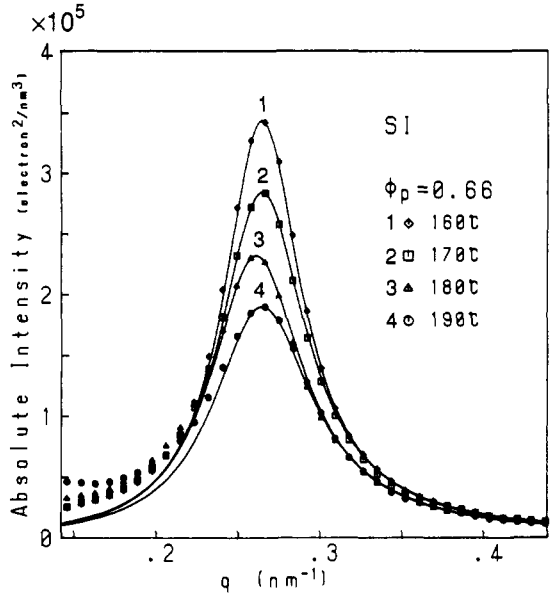

Figure 1. SAXS profiles in the disordered state for the DOP solution of pure SI (ϕ_p = 0.66) at various temperatures.

DP of SI, and ν = $^1/_2$ and $^3/_5$ for the Θ and swollen coils, respectively. For the Θ condition, $\phi_{C,SI}$ = 0.0087, and thus our systems are in the high polymer concentration region where the SI molecules are highly overlapped with one another and also with the HS molecules (Table II). In most of the systems studied here, the volume fraction of HS, $\phi_P\phi_{HS}$, in the system SI/HS/DOP is also much greater than the corresponding overlap volume concentration $\phi_{C,HS} = N_{HS}^{-(3\nu-1)}$ = 0.32, 0.20, 0.14, 0.09, and 0.07 for S01, S02, S04, S10, and S17, respectively, for ν = $^1/_2$, except for the systems SI/S01 80/20 (ϕ_P = 0.74), SI/S02 80/20 (ϕ_P = 0.74), and SI/S04 80/20 (ϕ_P = 0.66) for which $\phi_P\phi_{HS} < \phi_{C,HS}$ (Table II). Here N_{HS} is the DP for HS.

The DOP solutions of SI and SI/HS were prepared as follows. A prescribed amount of polymer (or polymers) and DOP were first dissolved with an excess of dichloromethane, and the homogeneous solutions containing 10 wt % of the polymer (or the polymers) and DOP were prepared. The solutions were cast into films in Petri dishes by evaporating dichloromethane. The films containing DOP were further dried under vacuum until the specimens were at constant weight. After the evaporation, the specimens were weighed again to determine the total polymer concentrations listed in Table II.

The SAXS measurements were carried out as a function of temperature. The apparatus and methods were described in detail elsewhere.[18-20] Cu Kα radiation with the wavelength λ_r = 1.54 Å was used. The SAXS profiles were corrected for absorption, air scattering, background scattering arising from the thermal diffuse scattering (TDS), and slit-height and slit-width smearings.

III. Results

Figure 1 shows the SAXS profiles of the neat block copolymer SI with ϕ_p = 0.66 at various temperatures T in the disordered state (the single-phase state). The measured SAXS profiles were shown by the data points. The solid lines are the best-fitted theoretical profiles, which will be discussed later. Each profile has a maximum intensity at a scattering angle 2θ = 22.7 (min) (defined as $2\theta_m$), corresponding to q_m = 0.269 nm^{-1}, where q_m is a magnitude of scattering vector $\mathbf{q}$ at $2\theta = 2\theta_m$

$$|\mathbf{q}| = (4\pi/\lambda_r) \sin\theta \quad (1)$$

$2\theta_m$ or q_m does not change with increasing T above 160 °C but the intensity maximum $I_m \equiv I(q_m)$, the scattered intensity at $q = q_m$, decreases with T. Upon decreasing T below 160 °C, I_m further increases and q_m starts to shift toward smaller q_m as previously reported.[6,8,15] These T dependencies on q_m and I_m suggest that the block copolymer is in the disordered and ordered state at $T >$ 160° and at $T <$ 160 °C, respectively. A detailed discussion on T dependence of q_m below and above T_{ODT} will be given elsewhere.[21] A brief discussion on the change of q_m below and above ODT will be given in section IV-2 in conjunction with the chain stretching in the disordered state near ODT.[43]

Figure 2 shows the SAXS profiles for the binary mixtures of SI/S01 with the compositions (a) 80/20 (ϕ_p = 0.74), (b) 50/50 (ϕ_p = 0.74), and (c) 20/80 (ϕ_p = 0.85). The composition designates weight percents of SI and HS in the mixture SI/HS. Only the profiles in the disordered states at higher temperatures ($T > T_{ODT}$) are shown, and the measured profiles are shown by the data points, while the solid curves are the best-fitted theoretical profiles as will be discussed later in sections IV-1 and -2. Again we found for each mixture that the value q_m is independent of T but I_m decreases with increasing T, the trends appropriate for scattering in the disordered state.

Figures 1 and 2 clearly indicate that there are systematic changes in I_m and q_m (or $2\theta_m$) with increasing amount of ϕ_{HS}. Here the quantity I_m/ϕ_p can be taken to normalize the difference of ϕ_p, as I_m is proportional to ϕ_p.[15,22,35-37] The former change is associated with the amplitude of thermally activated composition fluctuations in the single-phase state and hence the thermodynamical stability of the mixtures, i.e., $\Delta T = |T - T_S|$ where T_S is the spinodal temperature. The latter change is associated with the wavelength D_S of the dominant mode of the fluctuations

$$D_S = 2\pi/q_m \quad (2)$$

One can observe remarkable suppression of I_m with increasing ϕ_{HS}, so that the appreciable SAXS intensity for the systems with higher ϕ_{HS} can be observed only at lower temperatures or higher ϕ_p, implying a suppression of T_S or an increase in the stability of the mixtures with increasing ϕ_{HS}. The shift of q_m with ϕ_{HS} is less remarkable with S01 than that with other HSs as will be shown immediately below. Although not shown here, the scattering profiles were also measured for a series of the mixtures SI/S02/DOP (e.g., 80/20 (ϕ_P = 0.74), 65/35 (ϕ_P = 0.75), 50/50 (ϕ_P = 0.85), 35/65 (ϕ_P = 0.85), 20/80 (ϕ_P = 0.85)) as a function of temperature T. They could also be fitted nicely with the theoretical curves and had q and T dependencies very similar to those in Figure 2, except for the fact that the decrease of q_m with ϕ_{HS} is greater than that for SI/S01/DOP. It should be noted also that the decrease of I_m/ϕ_P with ϕ_{HS} at a given T ($>T_{ODT}$) is less than that for SI/S01/DOP.

Figure 3 shows SAXS profiles at various T's in the disordered state for the mixtures with the higher molecular weight HS, e.g., for SI/S04, SI/S10, and SI/S17 with various compositions. For these mixtures the shift of q_m or $2\theta_m$ with ϕ_{HS} is much clearer than that for SI/S01; the q_m decreases with ϕ_{HS}, and the rate of the decrease increases with increasing N_{HS}. On the other hand, the drop of I_m with ϕ_{HS} becomes less distinct with increasing N_{HS} (cf. Figures 1 and 3c,d). The thermodynamic stability of the systems is less enhanced with increasing N_{HS} within the range of N_{HS} covered in this experiment. These points will be discussed in a more quantitative manner in sections IV-3 and IV-4.

IV. Analyses and Discussions

1. Scattering Theory. The scattering theory from block copolymers in the disordered state was first given by Leibler[13] for monodisperse, symmetric, A–B diblock

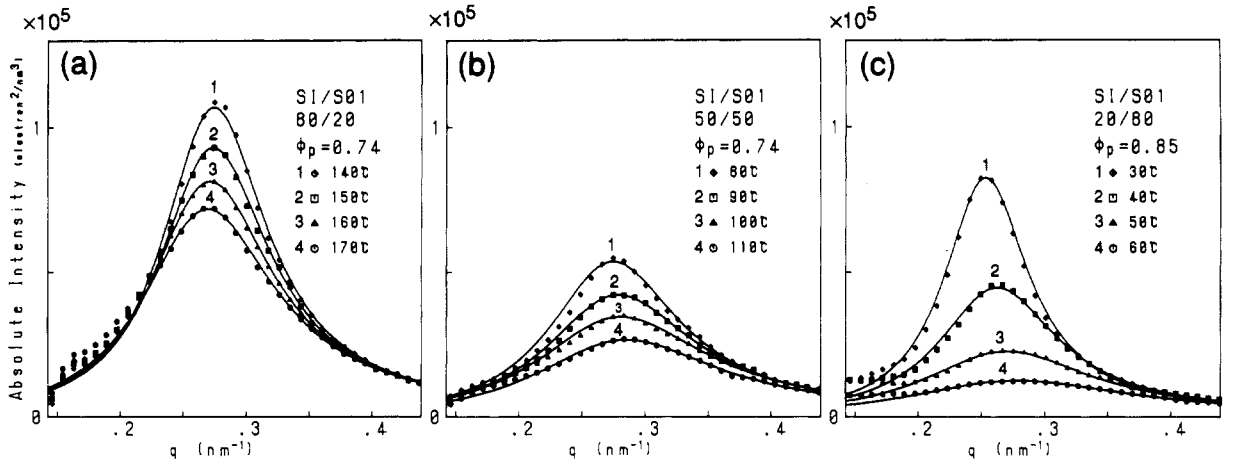

Figure 2. SAXS profiles in the disordered state for the DOP solutions of SI/S01 with compositions (a) 80/20 (ϕ_p = 0.74), (b) 50/50 (ϕ_p = 0.74), and (c) 20/80 (ϕ_p = 0.85) at various temperatures.

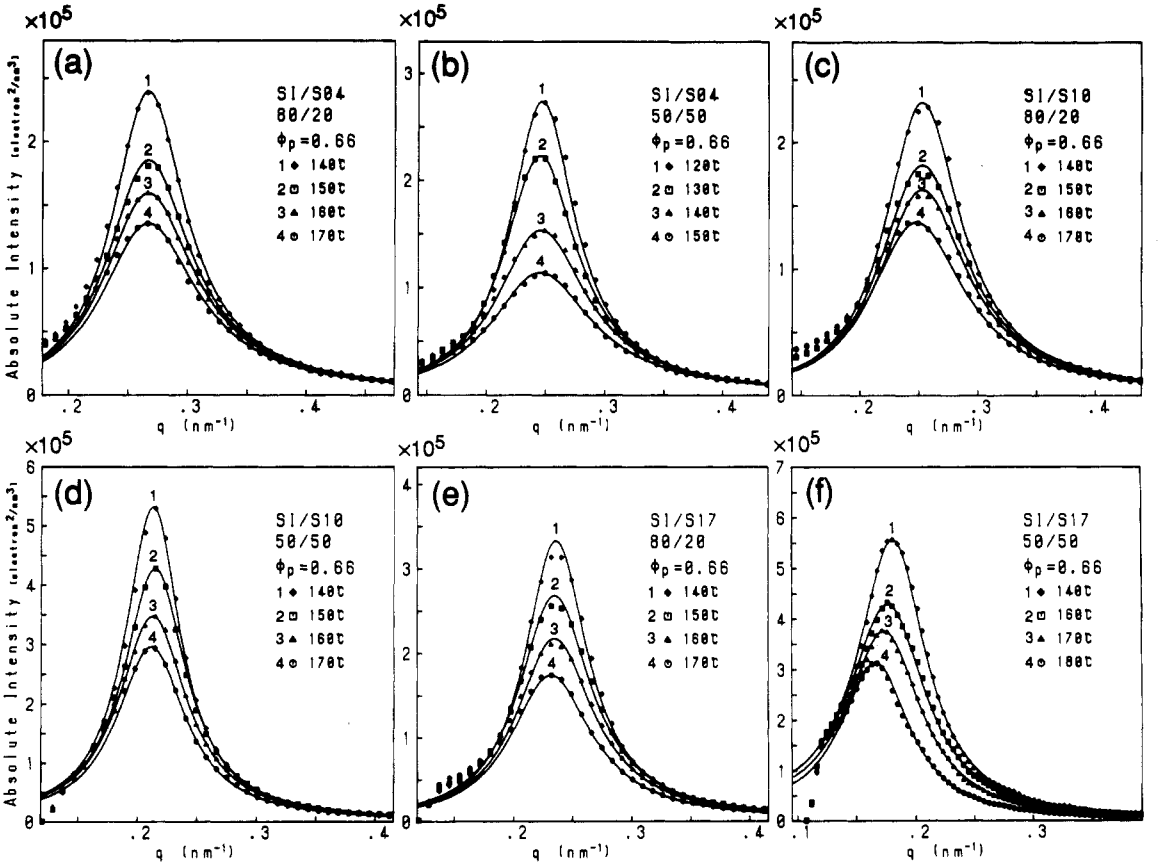

Figure 3. SAXS profiles in the disordered state for the DOP solutions of SI/S04 with (a) 80/20 and (b) 50/50, SI/S10 with (c) 80/20 and (d) 50/50, and SI/S17 with (e) 80/20 and (f) 50/50 at various temperatures. All the solutions have ϕ_p = 0.66.

copolymers based upon the mean-field random-phase approximation. Leibler's theory was generalized by Leibler and Benoit[23] and Benoit et al.[24] to symmetric copolymer/homopolymer blends. Recently we further generalized the scattering theory to asymmetric and polydisperse copolymer/homopolymer blends,[25] based on which we analyzed the measured scattering profiles discussed in section III. Here "symmetry" and "asymmetry" refer to Kuhn statistical lengths a_K and monomer volume v_K of the constituent polymers (K = A or B). For the symmetric block copolymers, $a_A = a_B$ and $v_A = v_B$, while for the asymmetric copolymers $a_A \neq a_B$ and $v_A \neq v_B$. Besides the corrections for the asymmetry and the polydispersity, the correction for the finite size effect was also introduced by Fredrickson and Helfand[26] for monodisperse, symmetric, and pure block copolymers using a method developed by Brazovskii.[27] The finite size effect was also considered by Burger et al.[28] for the polydisperse and symmetric copolymers. Here we neglect the finite size effect in our analyses, as the scattering theory that takes into account the finite size effect for polydisperse, asymmetric copolymer/homopolymer blends has not been developed at this moment. It is important to note that the finite size effect obviously affects the absolute values of χ determined by best fitting between theoretical and experimental SAXS profiles, generally increasing the absolute values of χ and its temperature dependence.[29]

Since the final formula for the scattering intensity $I(q)$ from the asymmetric and polydisperse mixtures of A–B block copolymer, A homopolymer, and B homopolymer (A–B/A/B) is lengthy, it will be summarized in the Appendix.

The scattering theory for the disordered melt was generalized to that for the block copolymer solutions in the disordered state.[35-38] The scattering theory for semidilute solutions of block copolymers was shown to be enormously simplified and given by

$$[I(q)/\phi_P]^{-1} \propto \overline{S(q)}/\overline{W(q)} - 2\chi_{eff} \quad (3)$$

in the context of the pseudobinary approximation.[31,38,39] The criteria for this approximation to be valid were examined elsewhere.[38] This approximation offers one-to-one correspondence between the melts and the solutions, in which the Flory interaction parameter χ, radius of gyration R_g, and scattering power $(a-b)^2$ in the melts are replaced by χ_{eff}, R_g, and $(a-b)_{eff}^2 = (a-b)^2\phi_P$ in the presence of the solvent, where a and b are the scattering lengths or electron densities of the constituent polymers A and B. Renormalization group analysis based on the blob picture gave detailed formula for χ_{eff} for the semidilute good[31,36,37] or Θ solvent.[31]

Our semidilute solutions satisfy the Θ condition, because $f_0 = (1-2\chi_{1S})/u^* \cong (1-2\chi_{2S})/u^*$ ($\cong$0.02) in ref 31 satisfies $f_0 \ll \phi_P$ (section II). Thus gyration radii appearing in eq 3 should be those for unperturbed chains.[40] χ_{eff} in eq 3 for the semidilute Θ condition is given by[31]

$$\chi_{eff} \cong \chi\phi_P^2/[\phi_P + \chi/u_{12}^*] \quad (4)^{41}$$

where χ is the bare interaction between the dissimilar segment units A and B and u_{12}^* ($\cong$10) is the fixed point given by eq 3.12 in ref 31. As will be shown later in section IV-5 and in Table III, χ varies from 0.03 to 0.09. Thus $\chi/u_{12}^* \cong 0.003$–$0.01$ and is much smaller than ϕ_P (=0.66–0.85). Under this weak-to-moderate segregation limit it follows that

$$\chi_{eff} = \chi\phi_P \quad (5)$$

In the following analysis on the SAXS profiles for the solutions in disordered state, we use eqs 3 and 5 and calculate $\overline{S(q)}/\overline{W(q)}$ using the gyration radii for the unperturbed coils.

2. Comparisons between Theoretical and Experimental Scattering Profiles. The theoretical scattering function $I(q)$ can be calculated by using the parameters λ, λ_D, $f_{A,n}$, $N_{K,n}$, and a_K (K = A, B, and D) as well as χ. Here λ is the heterogeneity index of the block chains ($\lambda_A = \lambda_B = \lambda$), which is related to the value $\lambda_t = M_w/M_n$ listed in Table I, i.e., the value measured for the SI block copolymer as a whole[32]

$$\lambda_t - 1 = (\lambda - 1)[f_{PS,n}^2 + (1-f_{PS,n})^2] \quad (6)$$

where $f_{PS,n}$ is the number-average volume fraction of PS block in SI (see eq A15). Using eq 6 we estimated λ as 1.14. $f_{PS,n}$ can be calculated from M_n, the composition of the SI block copolymer, and the mass densities d_{PS} and d_{PI} of pure PS and PI in the bulk; $d_{PS} = 1.052$ g/cm^3 and $d_{PI} = 0.925$ g/cm^3. λ_D is the heterogeneity index for HS and is given in Table I. $a_A = a_D \equiv a_{PS} = 0.68$ nm for PS[33] and $a_B \equiv a_{PI} = 0.59$ nm for polyisoprene.[34] It should be noted that d_{PI} and a_{PI} are the values for vinyl-rich polyisoprene. χ is used as an adjustable parameters. The reference volume v_0 was chosen as $v_0 = (v_{PS}v_{PI})^{1/2}$. The wavelength of the dominant mode of the fluctuations D_{ST} was estimated from the peak-scattering vector q_{mT} for the theoretical scattering profile by using

$$D_{ST} = 2\pi/q_{mT} \quad (7)$$

and this value was compared in Table II with the value D_S obtained experimentally from eq 2.

Table III
***A* and *B* Specifying the Temperature Dependence of $\chi = A + B/T$**

sample	comp, w/w %	A	B
SI		0.030 87	2.013
SI/S01	80/20	0.023 41	5.843
	50/50	0.024 46	10.38
	20/80	−0.024 19	35.85
SI/S02	80/20	0.031 11	2.358
	65/35	0.031 69	3.575
	50/50	0.030 32	5.125
	35/65	0.028 81	9.320
	20/80	0.010 07	24.16
SI/S04	80/20	0.031 41	2.931
	50/50	0.032 55	5.810
SI/S10	80/20	0.029 55	2.075
	50/50	0.035 13	1.096
SI/S17	80/20	0.027 38	1.953
	50/50	0.030 94	0.500

In reality we observed mismatches between q_m (the peak scattering vector for the experimental profile) and q_{mT}, as indicated in the disparity of $D_S/D_{ST} = q_{mT}/q_m$ from unity in Table II. Thus the theoretical peak position was first fitted with the experimental one by using R_{gn} also as an adjustable parameter where R_{gn} is the number-average radius of gyration of SI as a whole and defined by

$$R_{gn}^2 = R_{gPS,n}^2 + R_{gPI,n}^2 \quad (8)$$

The value of $R_{gK,n}$ (K = PS or PI) is the gyration radius of the corresponding block chain. Since we have the following relationships

$$R_{gPS,n}^2/R_{gn}^2 = [1 + (a_{PI}/a_{PS})^2(N_{PI,n}/N_{PS,n})]^{-1} \quad (9)$$

and

$$R_{gHS,n}^2/R_{gn}^2 = [N_{PS,n}/N_{HS,n} + (a_{PI}/a_{PS})^2(N_{PI,n}/N_{HS,n})]^{-1} \quad (10)$$

in which the quantities in the right-hand sides of eqs 9 and 10 are experimentally known, we can calculate the scattering profile and fit its peak position with the experimental one using R_{gn} as an adjustable parameter. After fitting the peak position, we further fit the entire shape of the theoretical scattering profile with that of the experimental one by adjusting χ_{eff}. From the value χ_{eff} thus estimated and eq 5, χ was determined and listed in Table III. Note that eqs 8–10 assume the SI block copolymer and HS homopolymer are Gaussian coils.

The theoretical profiles best fitted with the experimental profiles are shown by solid curves in Figures 1–3. We find good overall agreement between the experimental and theoretical profiles. There are slight deviations observed in small $q < q_m$ or q_{mT}, which may be attributed to experimental difficulties to obtain accurate data free from parasitic scattering in the small q's and/or to the concentration fluctuations of the solvent against polymers, i.e., to the nonzero osmotic compressibilities. These deviations should deserve future investigations and probably be best investigated by using a ultra-small-angle scattering apparatus such as a Bonse-Hart camera.[42] The experimental and theoretical peak scattering vectors agree also with an accuracy of 20% error as seen in the column $D_S/D_{ST} = q_{mT}/q_m$ of Table II. However, the experimental value of D_S is systematically greater than D_{ST} by 20% after averaging 60 data of D_S/D_{ST} in Table II.

The 20% disparity in D_S/D_{ST} or q_{mT}/q_m implies that SI and/or HS molecules are stretched 20% relative to the corresponding unperturbed chains, if the reported values of a_{PI} and a_{PS} are correct. The stretching may arise either from swelling of the SI block chains by the solvent and HS

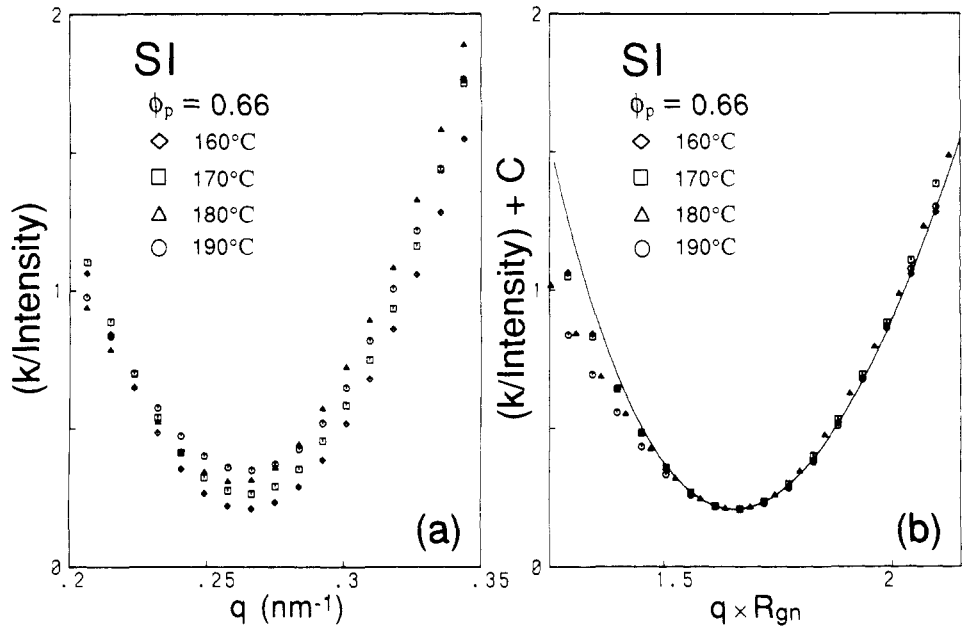

Figure 4. (a) $k/I(q)$ as a function of q at various temperatures, and (b) a master curve for $k/I(q) + C(T)$ as a function of qR_{gn} for pure SI ($\phi_p = 0.66$). k is a constant related to the absolute intensity, $C(T)$ is the temperature-dependent vertical shift factor, and R_{gn} is the number-average radius of gyration for the SI block copolymer.

homopolymers or from the stretching induced by the transition from the Gaussian to stretched coils in the disordered state near the ODT as reported by Almdal et al.[43] and Minchau et al.[44] The stretching due to the former is against our qualitative analysis, leading to a conclusion of SI and HS being in the semidilute Θ condition. If there is a problem in the qualitative analysis given in section II, it should be rigorously rechecked as a problem of chain stretching in the thermodynamically stable system SI/HS/DOP. The stretching due to the latter reason was claimed[43] to be as large as 13% relative to the Gaussian coil at the ODT, and this magnitude of the stretching is about equal to that found in our study.

This Gaussian–stretched coil transition[43] was found by changing the DP of the block copolymer (N) through the ODT at a fixed temperature T. In our experiments in which N is fixed but T is varied, this transition, if it occurs, should be observed in principle by changing χ and hence T, since changing N is equivalent to changing χ. In reality, however, over the temperature range covered, χ does not significantly change as will be shown later in section IV-5 and Table III, e.g., $(\chi_{ODT} - \chi_u)/\chi_{ODT}$ ($\cong$0.0074–0.0510) is much less than $(N_{ODT} - N_{GST})/N_{ODT} = 0.43$. Here χ_u and χ_{ODT} denote respectively the χ parameter at the upper limit of T covered in our experiment and that at ODT, and N_{ODT} and N_{GST} are respectively the value N at which the ODT occurs and that at which the Gaussian–stretched coil transition occurs. In other words, changing T shows much smaller effect on the changing χN (the segregation power) than on changing N. Thus in our case the degree of chain stretching in the disordered state, if it occurs, is essentially independent of T in the T range covered in our experiment, and this may provide a possible explanation why q_m and D_S are independent of T in the disordered state examined by our experiment. This speculation provides also a theoretical basis to identify the ODT as T at which q_m starts to decrease, even in the case when the chain stretching occurs in the disordered state near the ODT. The decrease of q_m with decreasing T below the ODT is due to chain stretching, which may be much stronger than that in the disordered state and which is induced by increasing segregation power as evidenced by the well-defined microdomain structure with a sharp interface.[45] We think that origin of the 20% disparity in D_S/D_{ST} and in the chain stretching in the disordered state is an open question that deserves future investigation.

From eq 3 it follows that

$$I(q) = (\text{const})[\overline{S(q)}/\overline{W(q)} - 2\chi_{eff}]^{-1} \qquad (11)$$

for the system with the small amount of DOP, where (const) is a proportionality constant used to fit the experimental and theoretical scattering profiles. Equation 11 can be rewritten as

$$k/I(q) = r_{C,n}\overline{S(q)}/\overline{W(q)} - 2\chi_{eff}r_{C,n} \qquad (12)$$

where k is the proportionality constant and $r_{C,n}$ is given by eq A18. Now $k/I(q)$ is associated with the free energy of the q-Fourier mode of the fluctuations. It comprises the q-dependent conformational term $r_{C,n}\overline{S(q)}/\overline{W(q)}$ and the q-independent interactional term $2\chi_{eff}r_{C,n}$. The constant term of the latter is obtained separately by best fitting with experimental and theoretical SAXS profiles as will be discussed in section IV-5 and as shown in Figures 1–3. Here we focus our attention on analysis of the q-dependent term. It should have a minimum value at $q = q_m$ (or q_{mT}). Moreover, its q dependence should be unaffected by the finite size effect discussed by Fredrickson and Helfand.[26] Its analysis is expected to provide a good test for the RPA theory. Since we have already found that R_{gn} or D_S values determined from q_m are larger than the unperturbed radii of gyration or D_{ST} by 20%, the q dependence of $k/I(q)$ was scaled with qR_{gn}. Then we can test the RPA theory on $I(q)$ in terms of the reduced wavenumber qR_{gn}.

Figure 4 shows the plot of $k/I(q)$ versus q (a) and $k/I(q) + C$ versus qR_{gn} (b) for the DOP solution of SI with $\phi_p = 0.66$ at various T's as indicated in the figure. As seen in part a, the curves $k/I(q)$ show a minimum at $q = q_m \cong 0.269$ nm^{-1}, and the wavenumber q_m is independent of T. The minimum value, which corresponds to $2(\chi_s - \chi_{eff})r_{C,n}$, decreases with decreasing T as χ_{eff} increases with decreasing T, where χ_s is the interaction parameter at the spinodal temperature. We are interested here in the q dependence of the term $\overline{S(q)}/\overline{W(q)}$ at various tempera-

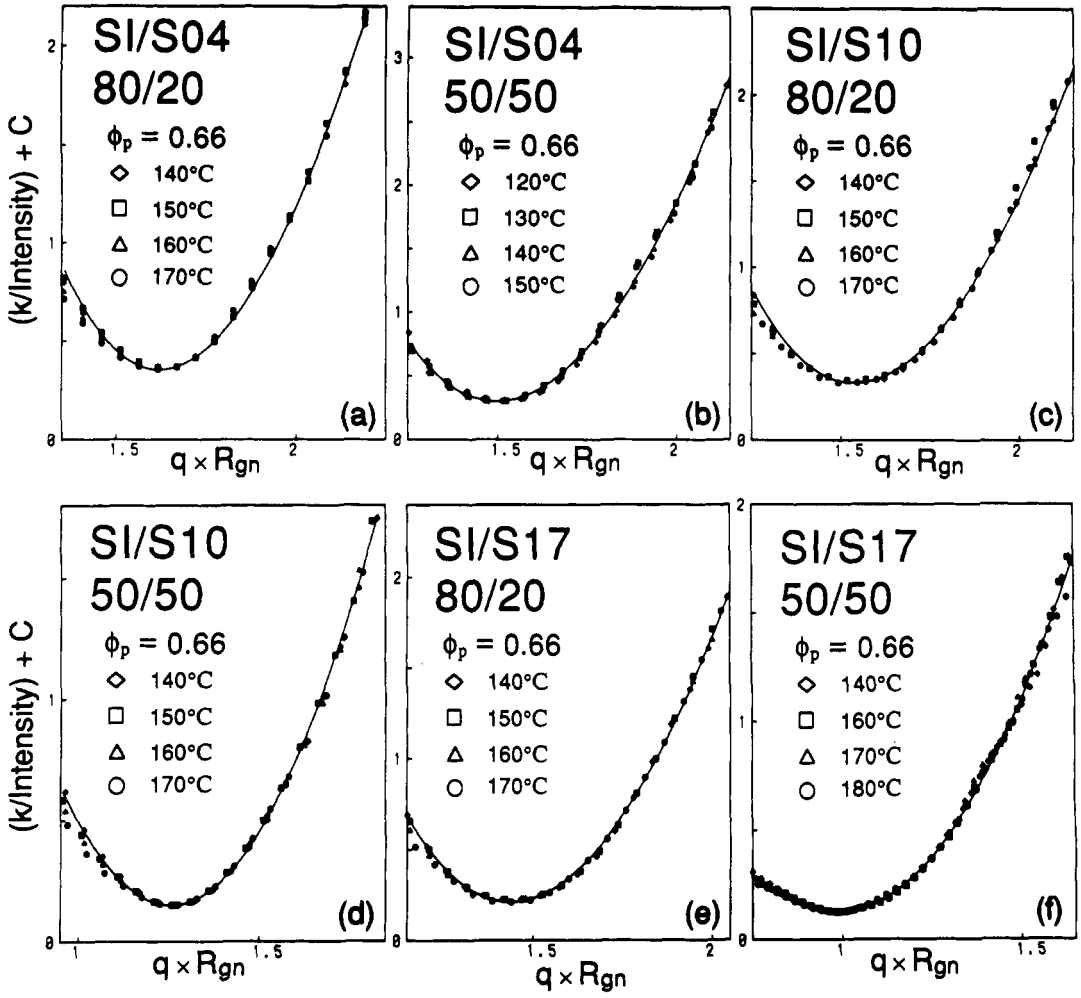

Figure 5. Master curves for $k/I(q) + C(T)$ as a function of qR_{gn} for SI/S04 with (a) 80/20 and (b) 50/50, SI/S10 with (c) 80/20 and (d) 50/50, and SI/S17 with (e) 80/20 and (f) 50/50. All the systems have $\phi_p = 0.66$. $C(T)$ and R_{gn} have the same meaning as in Figure 4.

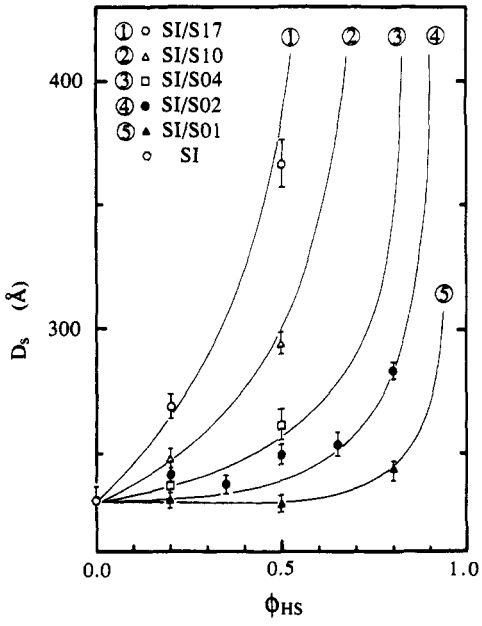

Figure 6. Wavelengths D_S of the dominant mode of the thermal composition fluctuations as a function of volume fraction of ϕ_{HS} for the binary mixture SI/HS. The solid lines show the theoretical results obtained by the RPA theory.

tures and in how the q dependence is affected by temperature. Therefore each curve in part a was shifted vertically to the curve obtained at the lowest temperature, e.g., that at $T = 160$ °C, the result of which is shown in part b, where C is the temperature-dependent shift factor, and q is also scaled by R_{gn} given by eq 8, where the unperturbed chain dimensions were used for $R_{gK,n}$ and $R_{gK,n}$ was assumed to be independent of T. It should be noted that the temperature dependence of the shift factor was obtained from the temperature dependence of $\chi_{eff} = \chi\phi_p$ where the temperature dependence of χ is shown in Table III (see section IV-5). The experimental curves obtained at different T's approximately superpose on one another and fit also the theoretical curve based upon the RPA theory (the solid line), except the slight deviations seen at the small- and large-q limits in Figure 2b, at which the intensity $I(q)$ is relatively low and hence $k/I(q)$ may be subjected to greater error.

The experimental master curves $k/I(q) + C$ were also obtained for other systems and they were found to agree reasonably well with the theoretical curves (the solid lines) for the range of molecular weight and weight fraction of homopolymers covered in our experiments, as shown in Figure 5 as representative examples, assuring validity of the RPA theory used in our study, except for the disparity in R_{gn} by 20%. All the results for SI/S01 and SI/S02 were also in good agreement with the theoretical curves, though they are not shown here. From the results shown in Figures 4 and 5, it is concluded that the q dependence is scaled with temperature-independent R_{gn} and that the chain stretching of the coils in the disordered state, if it exists, is independent of T covered in this experiment.

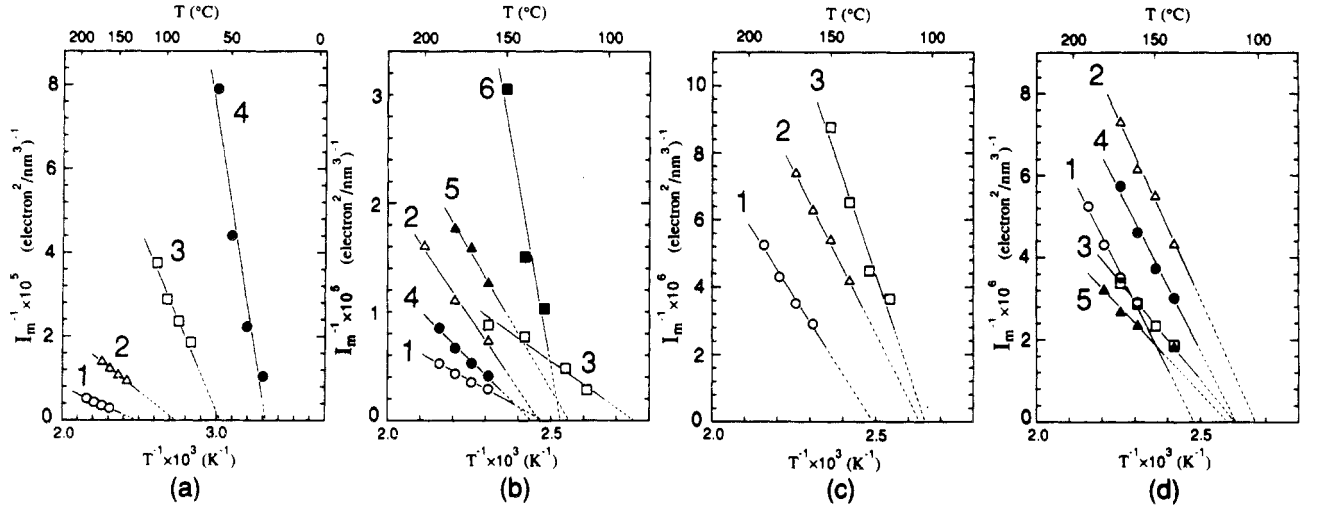

Figure 7. I_m^{-1} versus T^{-1} for various mixtures. (a) 1, SI (ϕ_p = 0.66); 2, SI/S01 80/20 (ϕ_p = 0.74); 3, SI/S01 50/50 (ϕ_p = 0.74); 4, SI/S01 20/80 (ϕ_p = 0.85). (b) 1, SI (ϕ_p = 0.66); 2, SI/S02 80/20 (ϕ_p = 0.74); 3, SI/S02 65/35 (ϕ_p = 0.75); 4, SI/S02 50/50 (ϕ_p = 0.85); 5, SI/S02 35/65 (ϕ_p = 0.85); 6, SI/S02 20/80 (ϕ_p = 0.85). (c) 1, SI (ϕ_p = 0.66); 2, SI/S04 80/20 (ϕ_p = 0.66); 3, SI/S04 50/50 (ϕ_p = 0.66). (d) 1, SI (ϕ_p = 0.66); 2, SI/S10 80/20 (ϕ_p = 0.66); 3, SI/S10 50/50 (ϕ_p = 0.66); 4, SI/S17 80/20 (ϕ_p = 0.66); 5, SI/S17 50/50 (ϕ_p = 0.66).

3. Wavelength D_S (or D_{ST}) of the Dominant Mode of the Fluctuations. The wavelengths D_S of the dominant mode of the fluctuations listed in Table II for the various mixtures are plotted as a function of ϕ_{HS} in Figure 6 where the solid lines show the theoretical wavelengths D_{ST} obtained by setting R_{gn} = 60.6 Å. It should be noted here that the values of D_S were found to be independent of ϕ_p for the high concentrations covered in our experiment.[40]

We can find the following general trends. (i) For HS with a given molecular weight, D_S tends to increase with increasing HS fraction, except for the HS with the lowest molecular weight, e.g., S01, for which D_S first remains constant upon increasing HS and then increases with a further increase of HS. (ii) For a given fraction of HS, D_S increases with increasing N_{HS}. (iii) The experimental variations of D_S with ϕ_{HS} and N_{HS} can be well described by the RPA theory.

4. Spinodal Point. According to the mean-field RPA theory given by eq 11 or 12, the reciprocal peak scattered intensity $I_m^{-1} \equiv I(q_m)^{-1}$ linearly decreases with χ_{eff} and becomes zero at the spinodal point, satisfying

$$2\chi_{eff,S} = \overline{S(q_m)}/\overline{W(q_m)} \quad (13)$$

Since the temperature dependence of χ_{eff} is given by

$$\chi_{eff} = A' + B'/T \quad (14)$$

as will be discussed later in section IV-5 and shown in Figure 9, I_m^{-1} should linearly decrease with $1/T$ and become zero at the mean-field spinodal temperature T_S'. The temperature T_S' for the DOP solution was converted to the temperature T_S for the mixtures in bulk by using eq 5, $\chi_{eff,S} = A' + B'/T_S' \equiv (A + B/T_S)\phi_P$, where A and B are defined by

$$\chi = \chi_{eff}/\phi_p = (A'/\phi_p) + (B'/\phi_p)/T \equiv A + B/T \quad (15)$$

Figure 7 shows the plot of I_m^{-1} versus T^{-1} and the corresponding mean-field T_S'. It is found that I_m^{-1} is approximately linear to T^{-1}, except for small deviations as seen by the concave curvatures, which may be attributed to the finite size effect.[26,47] Thus T_S' or T_S estimated is an approximate value. It should be noted here that a theory that accounts for the finite size effect does not exist for the binary mixtures of HS/SI. A generalization of the theory for such systems with relatively low molecular weights is badly needed. Figure 8 shows the "mean-field spinodal temperature" T_S thus determined as a function of ϕ_{HS} and N_{HS}. A pronounced decrease in T_S is seen with increasing amount of the small molecular weight HS (see curves no. 4 and 5 for SI/S02 and SI/S01, respectively). However, the effect of HS on T_S is much smaller and more complex for the higher molecular weight HS, e.g., curves no. 1–3 for the mixtures with S17, S10, and S04, respectively. For these systems, there is a tendency such that T_S first decreases with ϕ_{HS} and then increases with a further increase of ϕ_{HS}. This trend is qualitatively in agreement with that predicted by Whitmore and Noolandi.[46]

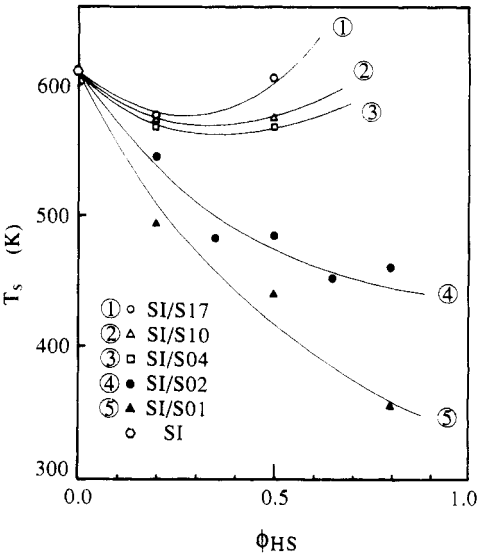

Figure 8. Mean-field spinodal temperature T_S as a function of the volume fraction of HS for binary mixtures SI/HS in the bulk.

5. χ Parameters as a Function of T, N_{HS}, and SI. Flory interaction parameter χ between PS and PI per segment in bulk was estimated from χ_{eff}, using eq 5, and the temperature dependence of χ is summarized in Table III.

Figure 9 shows the plots of χ as a function of $1/T$ (K^{-1}) for (a) SI/S01, (b) SI/S02, (c) SI/S04, and (d) SI/S10 and SI/S17. The following general features are found. (i) χ strikingly depends on ϕ_{HS}, increasing with increasing ϕ_{HS}.

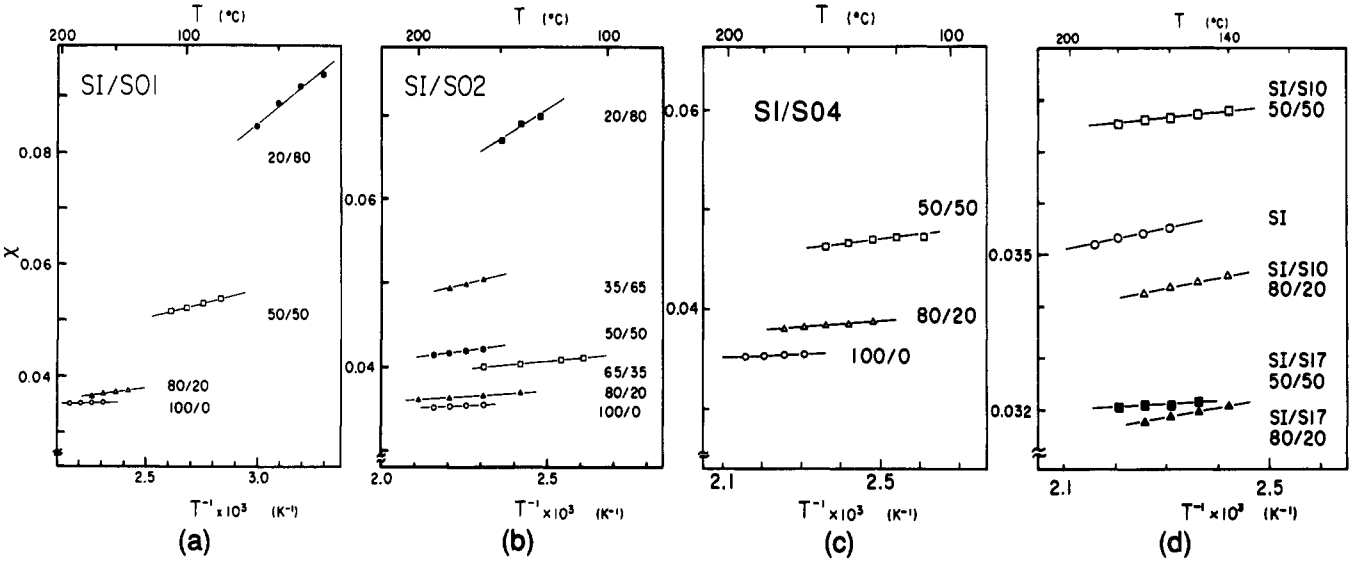

Figure 9. Temperature dependence of χ, the Flory interaction parameter between polystyrene and polyisoprene per segmental base, for (a) SI/S01, (b) SI/S02, (c) SI/S04, and (d) SI/S10 and SI/S17.

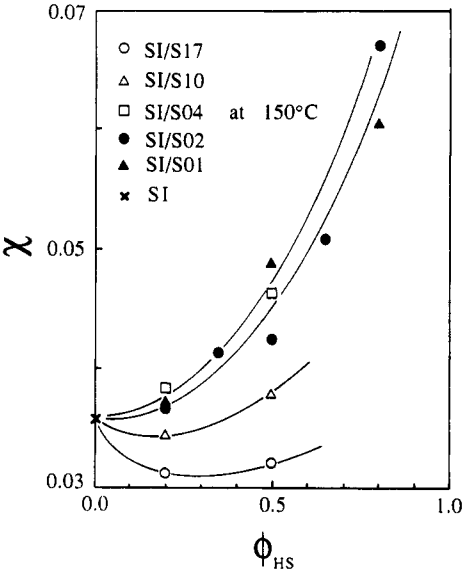

Figure 10. χ at 150 °C as a function of ϕ_{HS} for binary mixtures SI/HS.

(ii) χ remarkably depends on N_{HS} as well, decreasing with increasing N_{HS}. (iii) χ has the temperature dependence given by eq 15 in the narrow temperature range covered in our experiments. The dependence of χ on ϕ_{HS} is rather simple for HS with low molecular weights, e.g., for S01, S02, and S04, but complex for HS with the high molecular weights, e.g., for S10 and S17. A close observation of the latter tends to indicate that the value χ first decreases with ϕ_{HS} and then increases with a further increase of ϕ_{HS}. Figure 10 shows more directly the dependence of χ on ϕ_{HS} at a particular temperature, 150 °C.

Figure 11 shows the variations of the enthalpic (a) and entropic parts (b) of χ with ϕ_{HS}. The values A and B change remarkably with ϕ_{HS} for the mixtures with the low molecular weight HS (e.g., curves numbered 4 and 5) but less remarkably for the mixtures with the higher molecular weight HS (e.g., curves numbered 1–3). The variation of the quantities A and B with N_{HS} for the particular SI/HS mixtures with the compositions 80/20 and 50/50, for example, are rather systematic: (i) a systematic decrease of B and (ii) an initial increase of A, followed by a nearly constant value or a slightly decreasing one with increasing N_{HS}.

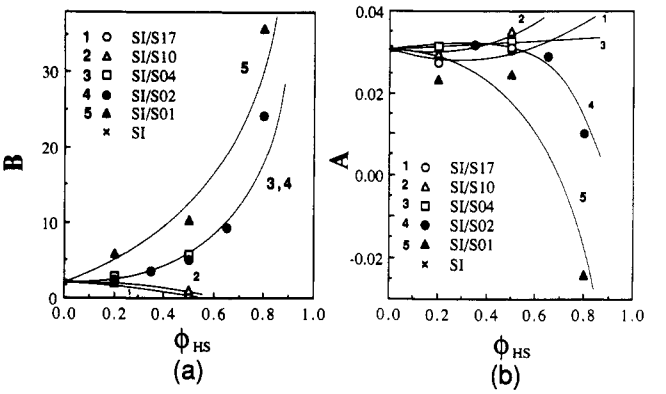

Figure 11. Enthalpic (B in part a) and entropic parts (A in part b) of χ as a function of ϕ_{HS} for binary mixtures SI/HS.

V. Concluding Remarks

The generalized RPA theory on elastic scattering from multicomponent systems in the disordered state was critically tested for binary mixtures of a SI block copolymer having a given molecular weight and HS having various degrees of polymerization N_{HS}. The RPA theory generalized for the asymmetry in monomer volumes and the polydispersity in molecular weights was found to explain well the q dependence of the experimental SAXS intensity, $I(qR_{gn})$, and the q dependence of the free energy associated with q-Fourier mode, i.e., $\overline{S(qR_{gn})}/\overline{W(qR_{gn})}$ in terms of the reduced q scale of qR_{gn}, as well as the variations of the wavelength of the dominant mode of the thermal composition fluctuations D_S with N_{HS} and ϕ_{HS}. A main disagreement from the RPA prediction should be noted here again: the predicted wavenumber q_{mT} for the scattering maximum is larger than the experimental wavenumber q_m by 20%. This disparity by 20% in our experiment was found to be essentially independent of T, ϕ_{HS}, and N_{HS} in the ranges of these parameters covered in our experiments. Nevertheless, the scattering method enables us to determine precisely the Flory interaction parameter χ between polystyrene and polyisoprene. The χ values obtained showed remarkable and interesting variations with ϕ_{HS} and N_{HS}. The mean-field spinodal temperature T_S was also found to depend markedly on N_{HS} and ϕ_{HS}.

Acknowledgment. This work is partially supported by a Grant-in-Aid for Scientific Research in Priority Areas "New Functionality Materials Design, Preparation and Control" (No. 02205066) from the Ministry of Education, Science and Culture, Japan, and by a scientific grant from the Mitsubishi Chemical Co. Ltd., Japan.

Appendix

The Scattering Intensity $I(q)$ from Asymmetric and Polydisperse Mixtures in the Disordered Melts. The final formula for scattering intensity $I(q)$ from the asymmetric and polydisperse mixtures of A–B block copolymer, A homopolymer, and B homopolymer (A–B/A/B) in melt is given by[25]

$$I(q)^{-1} \propto \overline{S(q)}/\overline{W(q)} - 2\chi \tag{A1}$$

where

$$\frac{\overline{S(q)}}{\overline{W(q)}} \equiv \frac{\overline{S_{\alpha\alpha}(q)} + \overline{S_{\beta\beta}(q)} + 2\overline{S_{\alpha\beta}(q)}}{\overline{S_{\alpha\alpha}(q)S_{\beta\beta}(q)} - \overline{S_{\alpha\beta}(q)}^2} \tag{A2}$$

$\overline{S_{ij}(q)}(i,j = \alpha,\beta)$ is given by

$$\overline{S_{\alpha\alpha}(q)} = \phi_c\langle r_c g^C{}_{AA}(q,-q)\rangle_v + \phi_D\langle r_D g^D{}_{DD}(q,-q)\rangle_v \tag{A3}$$

$$\overline{S_{\alpha\beta}(q)} = \overline{S_{\beta\alpha}(q)} = \phi_c\langle r_c g^C{}_{AB}(q,-q)\rangle_v \tag{A4}$$

$$\overline{S_{\beta\beta}(q)} = \phi_C\langle r_c g^C{}_{BB}(q,-q)\rangle_v + \phi_E\langle r_E g^E{}_{EE}(q,-q)\rangle_v \tag{A5}$$

where $\langle\ \rangle_v$ designates a volume average for the polydispersity effect, and the line over a quantity, e.g., $\overline{S_{\alpha\beta}(q)}$, indicates that it contains volume-averaged quantities. To simplify the notation we denote homopolymers A and B as D and E, respectively, and the copolymer as C. Thus ϕ_C, ϕ_D, and ϕ_E are the volume fractions of the corresponding species ($\phi_C + \phi_D + \phi_E = 1$). The quantity r_K (K = A, B, C, and D) is the "effective degree of polymerization" defined as

$$r_K = (v_K/v_0)N_K \tag{A6}$$

where v_K is the segmental volume of K, v_0 is the reference volume (the cell volume) used in defining the Flory interaction parameters, and

$$r_C = r_A + r_B \tag{A7}$$

the total effective DP for block copolymers. $g^C{}_{AA}$, $g^C{}_{AB}$, and $g^C{}_{BB}$ are Fourier transforms of the density–density correlations within a block chain A, between A and B block chains, and within a block chain B, respectively, while $g^D{}_{DD}$ and $g^E{}_{EE}$ are those for homopolymers D and E, respectively. The details can be found in ref 25.

We treat the polydispersity effect using a Schultz–Zimm distribution function after Leibler–Benoit[23]

$$\Psi_K(N_K) = \frac{1}{\Gamma(k_K+1)}\nu_K{}^{k_K+1}N_K{}^{k_K}\exp(-\nu_K N_K) \tag{A8}$$

where

$$\nu_K = k_K/N_{K,n} = (k_K+1)/N_{K,w} \tag{A9}$$

or

$$N_{K,w}/N_{K,n} = (k_K+1)/k_K \equiv \lambda_K \tag{A10}$$

$N_{K,n}$ and $N_{K,w}$ are the number-average and weight-average DP's of the K chain and λ_K is the heterogeneity index. The constants k_K and ν_K characterizes the polydispersity in molecular weight for the K chain. We assume that k_K and ν_K for A, B, D, and E are mutually independent, as in the previous treatments. Note that $\Psi_K(N_K)$ given by eqs A8 and A9 is the normalized weight distribution function.

For homopolymer, the volume average is equivalent to a weight average and can be written (for homopolymer D) by using the weight distribution function given by eq A8

$$\langle r_D g^D{}_{DD}(q,-q)\rangle_v = \int dN_D\ \Psi_D(N_D) r_D g^D{}_{DD}(q,-q) \tag{A11}$$

$$\langle r_D g^D{}_{DD}(q,-q)\rangle_v = \frac{2r_{D,n}}{x_{D,n}{}^2}\{x_{D,n} - 1 + [1 + (\lambda_D - 1)x_{D,n}]^{-1/(\lambda_D-1)}\} \tag{A12}$$

with an equivalent equation for homopolymer E. $x_{D,n}$ is defined in eq A19. For polydisperse and asymmetric copolymers, the volume and weight fractions are not equivalent, but we approximate the volume average by the weight average. Thus we have, for example

$$\langle r_c g^C{}_{AA}(q,-q)\rangle_v \cong \int dN_A\, dN_B\, \Psi_A(N_A)\Psi_B(N_B) r_c g^C{}_{AA}(q,-q) \tag{A13}$$

$$\langle r_c g^C{}_{AA}(q,-q)\rangle_v = \frac{2r_{C,n}f_{A,n}{}^2}{x_{A,n}{}^2}\left\{\frac{x_{A,n}}{2f_{B,n}}F\left(1, k+2, 2k+3; 1 - \frac{f_{A,n}}{f_{B,n}}\right) + \frac{1}{f_{B,n}}\frac{1}{\lambda+1}\left[z_2{}^{\lambda/(\lambda-1)}F\left(1, k+1, 2k+2; 1 - \frac{f_{A,n}}{f_{B,n}}z_2\right) - F\left(1, k+1, 2k+2; 1 - \frac{f_{A,n}}{f_{B,n}}\right)\right]\right\} \tag{A14}$$

for

$$f_{A,n} \equiv N_{A,n}v_A/[N_{A,n}v_A + N_{B,n}v_B] \le k_A/(k_A + k_B) \tag{A15}$$

where

$$z_2 = [1 + x_{A,n}(\lambda - 1)]^{-1} \tag{A16}$$

$$f_{B,n} = 1 - f_{A,n} \tag{A17}$$

$$r_{C,n} = (v_A/v_0)N_{A,n} + (v_B/v_0)N_{B,n} \tag{A18}$$

and

$$x_{K,n} = y_K N_{K,n} \quad (K = A, B, D) \tag{A19}$$

with

$$y_K = a_K{}^2 q^2/6 \tag{A20}$$

The condition stated by eq A15 arises from the convergence condition of the Laplace transformation of the Whittaker function.[30] The expression corresponding to the condition $f_{A,n} > k_A/(k_A + k_B)$ can be obtained similarly. $f_{K,n}$ is the volume fraction of K block chain based upon the number-average DP, $N_{K,n}$. Equation A14 was obtained for A–B copolymers having $k_A = k_B = k$ or $\lambda_A = \lambda_B = \lambda$ in eqs A9 and A10. In this case eq A14 can always be used by choosing the block chain having its average volume fraction $f_{K,n}$ less than $^1/_2$ as the A block chain. $F(\alpha, \beta, \gamma; z)$ is the Gauss hypergeometric function. In eq A12, $r_{D,n}$ is the number-average DP

$$r_{D,n} = (v_K/v_0)N_{D,n} \tag{A21}$$

$x_{D,n}$ is given by eqs A19 and A20 (K = D), and λ_D is the heterogeneity index for homopolymer D, which may differ from that of the copolymer blocks ($\lambda_A = \lambda_B = \lambda$). Next

$$\langle r_c g^C_{BB}(q,-q)\rangle_v \cong \frac{2r_{C,n}}{x_{B,n}^2 f_{B,n}^2}\left[\frac{x_{B,n}}{2f_{B,n}}F\left(1, k+1, 2k+3; 1-\frac{f_{A,n}}{f_{B,n}}\right) - \frac{1}{f_{B,n}}\frac{1}{\lambda+1}F\left(1, k+1, 2k+2; 1-\frac{f_{A,n}}{f_{B,n}}\right) + G_1\right] \quad (A22)$$

where

$$G_1 = \frac{z_5^{1/(\lambda-1)}}{f_{B,n}(\lambda+1)}F\left(1, k+1, 2k+2; 1-\frac{f_{A,n}}{f_{B,n}}z_5^{-1}\right) \quad (A23)$$

for

$$x_{B,n} \le k f_{B,n}(1/f_{A,n} - 1/f_{B,n}) \quad (A24)$$

and

$$G_1 = \frac{z_5^{\lambda/(\lambda-1)}}{f_{A,n}(\lambda+1)}F\left(1, k+1, 2k+2; 1-\frac{f_{B,n}}{f_{A,n}}z_5\right) \quad (A25)$$

otherwise. In these equations

$$z_5 = [1 + x_{B,n}(\lambda-1)]^{-1} \quad (A26)$$

Finally

$$\langle r_c g^C_{BB}(q,-q)\rangle_v \cong \frac{r_{C,n}}{x_{A,n}x_{B,n}}f_{A,n}f_{B,n}\left\{\frac{1}{f_{B,n}(\lambda+1)}F\left(1, k+1, 2k+2; 1-\frac{f_{A,n}}{f_{B,n}}\right) - \frac{z_2^{\lambda/(\lambda-1)}}{f_{B,n}(\lambda+1)}F\left(1, k+1, 2k+2; 1-\frac{f_{A,n}}{f_{B,n}}z_2\right) - G_1 + G_2\right\} \quad (A27)$$

where

$$G_2 = \frac{z_2^{\lambda/(\lambda-1)}z_5^{1/(\lambda-1)}}{f_{B,n}(\lambda+1)}F\left(1, k+1, 2k+2; 1-\frac{f_{A,n}z_2}{f_{B,n}z_5}\right) \quad (A28)$$

for

$$f_{A,n}z_2/f_{B,n}z_5 \le 1 \quad (A29)$$

and

$$G_2 = \frac{z_2^{1/(\lambda-1)}z_5^{\lambda/(\lambda-1)}}{f_{A,n}(\lambda+1)}F\left(1, k+1, 2k+2; 1-\frac{f_{B,n}z_5}{f_{A,n}z_2}\right) \quad (A30)$$

otherwise.

These equations reduced to those given previously for the symmetric block copolymers (eqs 42–48 in ref 30).

The scattering theory described above is developed for the mixtures A–B/A/B in the disordered melt. For the binary mixtures A–B/A we simply set $\phi_E = 0$.

References and Notes

(1) Zin, W.-C.; Roe, R.-J. *Macromolecules* **1984**, *17*, 183.
(2) Mori, K.; Hasegawa, H.; Hashimoto, T. *Polym. J.* **1985**, *17*, 799.
(3) Bates, F. S.; Hartney, M. A. *Macromolecules* **1985**, *18*, 2478.
(4) Nojima, S.; Roe, R.-J. *Macromolecules* **1987**, *20*, 1866.
(5) Bates, F. S. *Macromolecules* **1987**, *20*, 2221.
(6) Hashimoto, T.; Ijichi, Y.; Fetters, L. J. *J. Chem. Phys.* **1988**, *89*, 2463.
(7) Marie, P.; Selb, J.; Rameau, A.; Gallot, Y. *Macromol. Chem. Macromol. Symp.* **1988**, *16*, 301.
(8) Ijichi, Y.; Hashimoto, T.; Fetters, L. J. *Macromolecules* **1989**, *22*, 2817.
(9) Owens, J. N.; Gancarz, I. S.; Koberstein, J. T.; Russell, T. P. *Macromolecules* **1989**, *22*, 3380.
(10) Owens, J. N.; Gancarz, I. S.; Koberstein, J. T.; Russell, T. P. *Macromolecules* **1989**, *22*, 3388.
(11) Connell, J. G.; Richards, R. W. *Macromolecules* **1990**, *23*, 1766.
(12) de Gennes, P.-G. *Scaling Concepts in Polymer Physics*; Cornell University: Ithaca, NY, 1979; *J. Phys. (Paris)* **1970**, *31*, 235.
(13) Leibler, L. *Macromolecules* **1980**, *13*, 1602.
(14) Hashimoto, T.; Mori, K.; Hasegawa, H., manuscript in preparation.
(15) See, for example: Hashimoto, T. In *Thermoplastic Elastomers*; Legge, N. R., Holden, G., Schroeder, H. E., Eds.; Hanser: Munich, Vienna, New York, 1987; pp 350–383.
(16) Tanaka, H.; Hasegawa, H.; Hashimoto, T. *Macromolecules* **1991**, *24*, 240.
(17) Hashimoto, T.; Tanaka, H.; Hasegawa, H. *Macromolecules* **1990**, *20*, 4378.
(18) Hashimoto, T.; Suehiro, S.; Shibayama, M.; Saijo, K.; Kawai, H. *Polym. J.* **1981**, *13*, 501.
(19) Fujimura, M.; Hashimoto, T.; Kawai, H. *Mem. Fac. Eng. Kyoto Univ.* **1981**, *43*, 224.
(20) Fujimura, M.; Hashimoto, H.; Kurahashi, K.; Hashimoto, T.; Kawai, H. *Macromolecules* **1981**, *14*, 1196.
(21) Tanaka, H.; Hashimoto, T. *Macromolecules*, in press.
(22) Hashimoto, T.; Kowsaka, K.; Shibayama, M.; Kawai, H. *Macromolecules* **1986**, *19*, 754. Hashimoto, T.; Shibayama, M.; Kawai, H. *Macromolecules* **1983**, *16*, 1093.
(23) Leibler, L.; Benoit, H. *Polymer* **1981**, *22*, 195.
(24) Benoit, H.; Wu, W.; Benmouna, M.; Mozer, B.; Bauer, B.; Lapp, A. *Macromolecules* **1985**, *18*, 986.
(25) Tanaka, H.; Sakurai, S.; Hashimoto, T.; Whitmore, M. D. *Polymer*, in press.
(26) Fredrickson, G. H.; Helfand, E. *J. Chem. Phys.* **1987**, *87*, 697.
(27) Brazovskii, S. A. *Sov. Phys. JETP* **1975**, *41*, 85.
(28) Burger, C.; Ruland, W.; Semenov, A. N. *Macromolecules* **1990**, *23*, 3339.
(29) Inoue, T.; Hashimoto, T., manuscript in preparation.
(30) Mori, K.; Tanaka, H.; Hasegawa, H.; Hashimoto, T. *Polymer* **1989**, *30*, 1389.
(31) Onuki, A.; Hashimoto, T. *Macromolecules* **1989**, *22*, 879.
(32) Ionescu, L.; Picot, C.; Duplessix, R.; Duval, M.; Benoit, H. *J. Polym. Sci., Polym. Phys. Ed.* **1981**, *19*, 1019.
(33) Ballard, D. G.; Wignall, G. D.; Schelten, J. *Eur. Polym. J.* **1973**, *9*, 965.
(34) Hashimoto, T.; Nakamura, N.; Shibayama, M.; Izumitani, A.; Kawai, H. *J. Macromol. Sci.-Phys. B* **1980**, *17*, 389.
(35) Benmouna, M.; Benoit, H. *J. Polym. Sci., Polym. Phys. Ed.* **1983**, *21*, 1227.
(36) Olvera de la Cruz, M. *J. Chem. Phys.* **1989**, *90*, 1995.
(37) Fredrickson, G.; Leibler, L. *Macromolecules* **1989**, *22*, 1238.
(38) Hashimoto, T.; Mori, K. *Macromolecules* **1990**, *23*, 5347.
(39) Hashimoto, T.; Shibayama, M.; Kawai, H. *Macromolecules* **1983**, *16*, 1093.
(40) In separate experiments,[14] the DOP solution of an SI block copolymer having M_n (=1.8 × 10⁴) lower than that for the SI used in this work showed that its q_m value is independent of ϕ_P over the concentration range studied $\phi_P \ge 0.37$, indicating that the block copolymer solution is in the Θ state.
(41) It should be noted that the definition of χ_{eff} in eq 3 is different from that in eq 3.17a of ref 31.
(42) Bonse, U.; Hart, M. *Z. Phys.* **1966**, *189*, 151; In *Small-Angle X-ray Scattering*; Brunberger, H., Ed.; Gordon and Breach: New York, 1967; p 121.
(43) Almdal, K.; Rosedale, J.; Bates, F. S.; Wignall, G. D.; Fredrickson, G. H. *Phys. Rev. Lett.* **1990**, *65*, 1112.
(44) Minchau, B.; Dunweg, B.; Binder, K., preprint.
(45) See, for example: Hashimoto, T.; Shibayama, M.; Fujimura, M.; Kawai, H. In *Block Copolymers*, Meier, D. J., ed.; MMI press: Harwood Academic Pub.: New York, 1983; p 63.
(46) Whitmore, M. D.; Noolandi, J. *Macromolecules* **1985**, *18*, 2486.
(47) Bates, F. S.; Rosedale, J. H.; Fredrickson, G. H. *Phys. Rev. Lett.* **1988**, *61*, 2229.

Registry No. SI (block copolymer), 105729-79-1; HS (homopolymer), 9003-53-6.